

Towards discontinuous Galerkin solution of multiphase flows

D. Regener Roig^{*1}, A. Crivellini², A. Colombo¹

¹Department of Engineering and Applied Sciences, University of Bergamo, Italy

² Department of Industrial Engineering and Mathematical Sciences, Polytechnic University of Marche, Italy

*Corresponding author: daniel.regener@unibg.it

Introduction

This project is devoted to the high-fidelity simulations of multiphase flows. Since the solutions of the multiphase models can present a wide range of scales, we constructed our solver using a modal discontinuous Galerkin (dG) method that is arbitrarily high-order and can seek for the solution in meshes composed of elements of any shape. In our path to the entropy-stable resolution of fully non-equilibrium models, we demonstrate the effectiveness of our proposed stabilization strategies and mass transfer formulation in a simpler model.

Modelling

We consider the multi-component compressible Euler model for two components and with a source term \mathbf{b} [1], which is related to the mass transfer between phases

$$\frac{\partial \mathbf{q}}{\partial t} + \frac{\partial \mathbf{f}(\mathbf{q})}{\partial x} = \mathbf{b}. \quad (1)$$

Where the conservative set and the physical flux are respectively

$$\mathbf{q} := [\alpha_g \rho_g, \alpha_l \rho_l, \rho \mathbf{u}, \rho e^t]^\top, \quad (2)$$

$$\mathbf{f} := [\alpha_g \rho_g \mathbf{u}, \alpha_l \rho_l \mathbf{u}, \rho(\mathbf{u} \times \mathbf{u}) + \mathbf{I}^{d \times d} p, (\rho e^t + p) \mathbf{u}]^\top, \quad (3)$$

and we close the model supplying it with the stiffened gas equation of state (EOS)

$$p_k(e_k, \rho_k) = (\gamma_k - 1) \rho_k (e_k - e_{0,k}) - \gamma_k p_{\infty,k} \quad (4)$$

for each phase k . Finally, the equilibrium restrictions of the model are mechanical equilibrium ($p_l = p_g = p$) and thermal equilibrium ($T_l = T_g = T$).

Numerical solution

We consider a solution space \mathbb{P}^K constructed by a hierarchical and orthonormal basis in the mesh element T , [2] s.t

$$\mathbb{P}^K = \{v_h \in L^2(\Omega) | v_h|_T \in \mathbb{P}^K(T), \forall T \in \mathcal{T}_h\}. \quad (5)$$

Hyperbolic part

We solve the hyperbolic part of the model using the modal dG method. By some manipulation, we obtain

$$\sum_{T \in \mathcal{T}_h} \frac{dQ_{k,j}}{dt} + \sum_{F \in \mathcal{F}_h} \int_F \llbracket \phi_j \rrbracket H_k(\mathbf{q}|_{K_+}, \mathbf{q}|_{K_-}, \mathbf{n}|_{K_+}) d\sigma + \sum_{T \in \mathcal{T}_h} \int_K \frac{\partial \phi_j}{\partial x_i} f_{k,i}(\mathbf{q}) d\Omega = \mathbf{0}, \quad (6)$$

Where $Q_{k,j}$ are the components of the vector of unknown degrees of freedom. The previous system is integrated in time using a third-order strong stability preserving explicit Runge-Kutta (R-K) method under a CFL condition. We consider the Rusanov flux for H .

Instantaneous mass transfer

From the state obtained in the previous step, we apply a $p - T$ relaxation procedure [1] looking for a \circ^* state defined by

$$\rho^* = \rho \quad e^* = e \quad \mathbf{u}^* = \mathbf{u} \quad g_1^* = g_2^*. \quad (7)$$

regardless of the EOS used, this set of conditions lead to a system of equations

$$\begin{cases} g_l(p, T) - g_g(p, T) = 0 \\ \alpha_l(p, T)\rho_l(p, T)e_l(p, T) + \alpha_g(p, T)\rho_g(p, T)e_g(p, T) - \rho_0 e_0 = 0. \end{cases} \quad (8)$$

The conservation of total mass has been used to obtain the volume fractions as function of p and T as

$$\alpha_g(p, T) = \frac{\rho_0 - \rho_l(p, T)}{\rho_g(p, T) - \rho_l(p, T)} \quad (9)$$

The system is solved for p and T using a Newton-Raphson method. If one of the phases vanishes i.e. $\alpha_k \rightarrow 0$, we impose a negligible volume fraction $\alpha_{lim} = 10^{-8}$ and exit the mass transfer step.

Stabilization techniques

To ensure numerical robustness and physical consistency in the presence of strong gradients and complex flow regimes, we employ the following stabilization techniques.

Shock capturing

We apply the shock capturing term of [3] designed for ideal gases to the stiffened gases. The objective is to reduce instabilities at material interfaces, adding the following term to the discretization

$$\int_K \varepsilon_w \left(\frac{\partial \phi_h}{\partial x_i} \right) \left(\frac{\partial q_h}{\partial x_i} \right) d\Omega, \quad (10)$$

where the shock sensor is

$$\varepsilon_w = C_{SC} (h_K^{SC})^2 \sum_{n=1}^3 \left(\frac{|S_n| + |D_n|}{\tilde{w}_n} \right) |d\tilde{q}_j| \left(\frac{h_K^{SC}}{\max(1, \kappa)} \right). \quad (11)$$

And is taken as the maximum value over the quadrature points on the element, and C_{SC} is a user-defined constant.

Positivity preserving strategy

We enforce the positivity of quantities that are physically defined to be non-negative by iteratively removing higher-order modes until positivity is achieved within the cell. The implementation of this procedure is computationally efficient due to the orthonormality of the basis functions

Results and Discussion

We now present two benchmark tests to evaluate the stability and accuracy of the proposed method. These cases involve strong discontinuities and phase change, making them well suited to demonstrate the effects of the chosen stabilization strategies.

Liquid-Vapour shock tube problem

It consists of a shock tube with a mixture of liquid water and water vapour. In Figure 1 it is shown that the presented shock capturing (qSC) applies dissipation at the contact interface, while a similar but pressure-based shock capturing (pSC) [4] does not. We denote the value of CSC following the name of the strategy used.

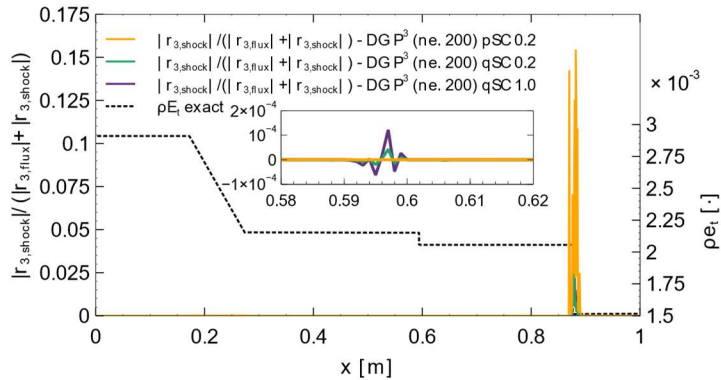


Figure 1. Results for the Liquid-Vapour shock tube problem with the same initial conditions as [1].

Depressurization of a CO₂ pipe

It is a shock tube problem where two distinct phases are present in the initial condition. Figure 2 presents the solutions both with and without mass transfer (MT). Reference numerical data from [1] has been extracted (digitized) directly from the original publication (---). When considering MT, the limiter is more active and affects at most the 4% of the elements per R-K stage.

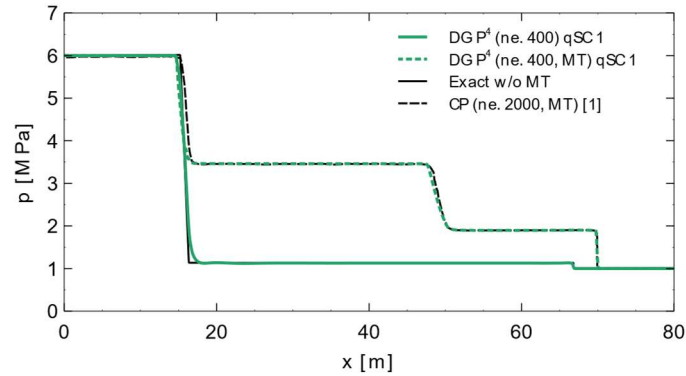


Figure 2. Results for the depressurization of a CO₂ pipe problem with the same initial conditions as [1].

Conclusion

The numerical method effectively handles mass transfer independently of the EOS and the results agree well with the literature. In our implementation, stabilization techniques were essential to prevent numerical failure during the simulation of 1D depressurization in a CO₂ pipe. While the results are encouraging, the positivity-preserving strategy remains intrusive and impacts the formal order of accuracy. Future developments will focus on extending the solver to multiple dimensions, eliminating the current equilibrium constraints, and reducing the impact of the positivity-preserving limiter.

Nomenclature

\mathbf{q}	Vector of conservative variables [various]	T	Element of the mesh [·]
\mathbf{f}	Physical flux vector [various]	\mathcal{T}_h	Set of elements of the mesh [·]
\mathbf{b}	Mass transfer source term [$\text{kg m}^{-3} \text{s}^{-1}$]	F	Face of the mesh [·]
\mathbf{x}	Space coordinates [m]	\mathcal{F}_h	Set of faces of the mesh [·]
α_k	Volume fraction of phase k [·]	Q	Solution vector [various]
ρ_k	Density of phase k [kg m^{-3}]	ϕ	Basis functions [·]
ρ	Mixture density [kg m^{-3}]	H	Numerical flux function [various]
\mathbf{u}	Mixture velocity [m s^{-1}]	K_+	External trace [·]
e^t	Total specific energy [$\text{J m}^3 \text{kg}^{-1}$]	K_-	Internal trace [·]
p_k	Pressure of phase k [Pa]	\mathbf{n}	Normal vector to F pointing outwards
e_k	Internal specific energy [$\text{J m}^3 \text{kg}^{-1}$]	ε_w	Shock sensor [·]
γ_k	Stiffened gas EOS constant [·]	h_K^{SC}	Element characteristic length [m]
$e_{0,k}$	Reference specific energy [$\text{J m}^3 \text{kg}^{-1}$]	S_n	Shock capturing term [various]
$p_{\infty,k}$	Stiffened gas EOS constant [Pa]	D_n	Shock capturing term [various]
T_k	Temperature of phase k [K]	\mathbf{w}_n^*	Corrected state vector for SC [various]
T	Mixture temperature [K]	\mathbf{w}_n	State vector vector for SC [various]
p	Mixture pressure [Pa]	$d\tilde{\mathbf{q}}_j$	Maximum normalized gradient of w_n [various]
κ	Polynomial degree of the solution space [·]	r	Residual of the spatial discretization [various]

References

- [1] Bacigaluppi, P., Carlier, J., Pelanti, M., Congedo, P. M., Abgrall, R., Journal of Scientific Computing. 90: 1 (2022).
- [2] Bassi, F., Botti, L., Colombo, A., Di Pietro, D.A., Tesini, P., Journal of Computational Physics 231: 45-65 (2012).
- [3] Franchina, N., Savini, M., Bassi, F., Journal of Computational Physics 315: 302-322 (2016).
- [4] Regener Roig, D., Crivellini, A., Colombo, A., Journal of Computational Physics 114808 (2026).